MICROBIAL IMPACTS TO THE NEAR-FIELD ENVIRONMENT GEOCHEMISTRY (MING): A MODEL FOR ESTIMATING MICROBIAL COMMUNITIES IN REPOSITORY DRIFTS AT YUCCA MOUNTAIN

DARREN M. JOLLEY[1] Duke Engineering and Services, 1180 Town Center Drive, Las Vegas, Nevada 89144

THOMAS F. EHRHORN[2] Duke Engineering and Services, One Park Square, 6501 Americas Parkway NE, Suite 810, Albuquerque New Mexico 87110

JOANNE HORN[3] Lawrence Livermore National Laboratory, 7000 East Ave., L-631, Livermore California 94550

Abstract

Geochemical and microbiological modeling was performed to evaluate the potential quantities and impact of microorganisms on the geochemistry of the area adjacent to and within nuclear waste packages in the proposed repository drifts at Yucca Mountain, Nevada. The microbial growth results from the introduction of water, ground support, and waste package materials into the deep unsaturated rock. The simulations, which spanned one million years, were accomplished using a newly developed computer code, **M**icrobial **I**mpacts to the **N**ear-Field Environment **G**eochemistry (MING). MING uses environmental thresholds for limiting microbial growth to temperatures below 120°C and above relative humidities of 90 percent in repository drifts. Once these thresholds are met, MING expands upon a mass balance and thermodynamic approach proposed by McKinley and others (1997), by using kinetic rates to supply constituents from design materials and constituent fluxes including solubilized rock components into the drift, to perform two separate mass-balance calculations as a function of time. The first (nutrient limit) assesses the available nutrients (C, N, P and S) and calculates how many microorganisms can be produced based on a microorganism stoichiometry of $C_{160}(H_{280}O_{80})N_{30}P_2S$. The second (energy limit) calculates the energy available from optimally combined redox couples for the temperature, and pH at that time. This optimization maximizes those reactions that produce >15kJ/mol (limit on useable energy) using an iterative linear optimization technique. The final available energy value is converted to microbial mass at a rate of 1 kg of biomass (dry weight) for every 64 MJ of energy. These two values (nutrient limit and energy limit) are then compared and the smaller value represents the number of microorganisms that can be produced over a specified time. MING can also be adapted to investigate other problems of interest as the model can be used in saturated and unsaturated environments and in laboratory situations to establish microbial growth limitations. Other projected uses include investigations of contaminated locations where monitored natural attenuation or engineered bioremediation could be employed.

[1] Email address: darren_jolley@ymp.gov, Fax #: 702-295-3554
[2] Email address: thomas_ehrhorn@ymp.gov
[3] Email Address: horn3@llnl.gov

Keywords: Geomicrobiology, Microbial Communities, Bioremediation, Biofilms, Engineered Barriers, Geochemistry, Predictive Modeling, Radionuclide Sorption

1. Introduction

In the potential Yucca Mountain Project (YMP) repository environment (Figure 1), located in southern Nevada, bulk and localized chemistry within the emplacement drifts may be affected by microbial activity. Large sources of potential nutrients and energy for microorganisms are found in the materials used in the construction of the ground support. The waste-package materials represent reduced metals that can be oxidized to provide energy for microorganisms, and the waste forms themselves contain both nutrient (when solubilized) and energy sources for organisms. These large quantities of materials would be emplaced in an environment that is currently nutrient limited (Keift et al. 1997, Horn et al. 2002)

With the introduction of additional nutrients and energy (in the form of electrons from reduced steels and alloys) sizeable microbial communities could develop that might potentially affect many different aspects of the in-drift geochemical environment. Various classes of microorganisms can thrive over a wide range of pH, under elevated hydrostatic pressures, in highly saline conditions, and at radiation levels that would be lethal to humans (Pedersen and Karlsson 1995). Additionally, microorganisms most often live in nutrient starved environments (Amy 1997; Morita 1990) where they may fix CO_2 as a source of cellular carbon (autotrophy), and obtain energy through the oxidation of H_2, N_2 and CH_4 directly from the gas phase (Keift and Phleps 1997). Microorganisms colonize surfaces thereby generating biofilms (Little et al. 1997) that contain microenvironments in which conditions are altered from that of the overall environment. Anaerobic niches occur within biofilms that allow anaerobic organisms to live under otherwise aerobic conditions. Biofilms and the metabolic processes that go on within them often induce localized corrosion of metal surfaces to which they are attached (Horn and Jones, 2002).

Microbial processes affecting radionuclide transformations include adsorption/precipitation, complexation/chelation, dissolution, oxidation/reduction reactions, and colloidal aggregation. Microbial heterotrophic aerobic respiration generates carbon dioxide as a metabolic endproduct, which also enables complexation of uranium and other radionuclides. These processes can act to affect radionuclide transport processes, in many instances causing increases in radionuclide solubility or transportability increasing the likelihood of nuclide transport away from the repository drifts. Additionally, microorganisms create microenvironments of nutrient and chemical gradients that are capable of altering radionuclide solubilities (Hersman 1997).

Because microbial processes can directly affect repository performance, an effort was made to predict the quantity of microbial biomass that could be generated through time as a result of emplacement of ground support and waste package materials along with the waste form itself. This effort resulted directly in the development of the **M**icrobial **I**mpacts to the **N**ear-field Environment **G**eochemistry (MING) software code (Ehrhorn and Jolley, 1998a, 1998b and O'Connell 1998).

2. Limits to microbial growth and metabolism

MING was designed to function within parameters that have been shown to directly affect microbial activity, including nutrient availability, salinity, pH, water activity, radiation, temperature, and redox conditions, coupled with relevant metabolic processes. Conditions such as relative redox, nutrients, water activity, and temperature are directly incorporated into MING; other parameters such as salinity, pH, size, and radiation are excluded from model and code development because their effects do not impact the results of the calculations if specific assumptions are made regarding the types of organisms that the environment will support. For example, MING assumes that halophiles take over if salt is high, acidophiles predominate if pH is low, and radioresistant organisms thrive when radiation dose is elevated (Jolley 2000, Ehrhorn and Jolley 1998a).

2.1 Redox conditions and metabolic processes

In deep unsaturated zones such as the potential repository in Yucca Mountain, a heterogeneous microbiological community can exist where many metabolic groups are represented (Hersman 1997), including heterotrophs, autotrophs, aerobes, facultative anaerobes, and anaerobes. While heterotrophs derive energy (as reducing equivalents) from reduced carbon compounds, other types of organisms use diverse reduced inorganic compounds as an energy source; and anerobes utilize oxidized species other than oxygen as terminal electron acceptors. Due to utilization of various redox pairs for deriving energy and as terminal electron sinks, microorganisms tend to accumulate at redox interfaces where both metabolic electron donors and electron acceptors are available. Metabolic processes which provide energy (as electrons) for growth include oxidation of reduced carbon compounds, nitrification which employs reduced nitrogen compounds as energy sources, hydrogen oxidation, methane oxidation, and manganese, sulfur and iron oxidation. Terminal electron acceptors include oxygen (aerobic respiration), oxidized nitrogen compounds (denitrification), sulfate, carbon dioxide (generating methane, methanogenesis), and ferric iron. Additionally, research has demonstrated microbes that use oxidized iron and manganese as electron acceptors are also capable of employing alternative oxidized species as terminal electron sinks. For example, several iron reducing species can also reduce U(VI) to U(IV) (Lovley et al. 1991, Lovley and Phillips 1992, Lovley

et al. 1993). This could play a potential role in the growth and persistence of microbial populations within a high level radioactive waste repository where the majority of the waste emplaced would be spent nuclear fuel. Table 1 gives a listing of redox half reactions that are used in MING.

2.2 Temperature

The temperature of the subsurface environment will affect or limit the type of bacteria present, based on the optimum growth temperatures of the organisms present. The maximum temperature at which known microorganisms can exist in an active state is 120°C (Pedersen and Karlsson 1995; Horn and Meike 1995). This value is thus the temperature threshold that MING uses to suspend microbial growth, and MING further assumes that all bacteria growing in the 50-120°C range are thermophiles. During the period of thermal perturbation resulting from waste package emplacement, the temperature in the repository drifts could exceed 120°C.

2.3 Water Availability

Water availability (or the activity of water a_w) is essential for microbial growth (Amy and Haldeman 1997; Banfield and Nealson 1997; Pedersen and Karlsson 1995). Most bacteria perish, sporate, or become dormant when a_w falls below about 0.90 and have difficulty thriving when a_w is less than 0.95 (Brown, 1976). In order for bacteria to grow well, a_w needs to be around 0.98 (Pedersen and Karlsson 1995). The relationship $a_w=RH/100$ is used to define water activity (absent ionic considerations). The availability of water for microbial growth in the unsaturated zone at Yucca Mountain will be dependent on thermohydrological conditions. During the thermal pulse caused by initial emplacement of radioactive, heat-generating waste packages, a_w values in the drift could approach zero. In order to account for this period where there is not enough moisture to allow microbial growth (a_w <0.90), growth is not initiated until the minimum activity of water has been reached. However, water activity in the potential repository is expected to approach 1.0 (relative humilities (RH) near 100 percent) as radionuclide decay progresses and temperatures decrease.

2.4 Nutrition

About 95 percent of the microbial cell dry weight is made up ten major elements: carbon, oxygen, hydrogen, nitrogen, sulfur, phosphorous, potassium, calcium, magnesium and iron (Amy and Haldeman 1997; Banfield and Nealson 1997; Pedersen and Karlsson 1995). Several trace elements are also found in the biomass, namely, manganese, zinc, cobalt, molybdenum, nickel and copper. These trace elements are needed in such low concentrations that they are not thought to be limiting factors in microbial growth. The requirements for carbon,

hydrogen, and oxygen are normally satisfied together, because they are the chief constituents of the molecules that make up reduced carbon sources for organisms.

Autotrophic and heterotrophic communities are found in the deep subsurface at Yucca Mountain. Heterotrophs show a great range of flexibility with respect to carbon compounds that can be utilized. Some bacteria are capable of degrading complex, substituted and stable carbon compounds (e.g., substituted aromatics and polymers), whereas others can only catabolize a few select carbon compounds. Autotrophs alternatively utilize carbon dioxide as a cellular carbon source. The fixation of CO_2 as a source of cellular carbon, however is an energetically expensive process.

In order to grow, organisms need to incorporate nitrogen, phosphorous, and sulfur (Amy and Haldeman 1997; Banfield and Nealson 1997; Pedersen and Karlsson 1995), as these elements are essential components of proteins, cofactors, nucleic acids, and phospholipids. Organisms usually employ inorganic sources of these elements. Nitrogen is often incorporated into cellular metabolism by reducing nitrate to ammonia, which then can be utilized by various biosynthetic pathways. Select groups of bacteria are able to reduce and assimilate atmospheric nitrogen. However, this process is extremely sensitive to oxygen levels, requires a great deal of available energy, and is most often associated with either marine organisms or those involved with plant symbioses. Almost all bacteria use inorganic phosphate as their phosphorous source and incorporate it directly. Most bacteria use sulfate as a source of sulfur and reduce it by assimilatory reduction. Sulfate is available in groundwater and is not usually a limiting nutrient, but low concentrations of phosphate and nitrogen can limit the growth of microorganisms. In the subsurface environment at Yucca Mountain, there is sufficient nitrogen in the groundwater. Under most conditions however, the flux of energy rather than the availability of nutrients will limit the amount of microbial growth possible.

3. Mathematical model

In developing a model that estimates the growth of microbial communities, three basic approaches are possible: mass balance, thermodynamic and kinetic. These approaches have been previously documented by McKinley and Grogan (1991), Capon and Grogan (1991), and Grogan and McKinley (1990). As a starting point, we chose to use an approach similar to that used by the Canadian High-Level Waste Repository program (Stroes-Gascoyne 1989) and the Swiss Low/Intermediate-Level Waste Repository program (Capon and Grogan 1991, McKinley and Grogan 1991 and McKinley et al. 1997) which use both mass balance and thermodynamics to quantify the impacts of microbial populations. We augmented this approach by directly accounting for the kinetic rate of supply of potential

nutrients and energy and the transient behavior of environmental conditions in a repository. In essence, the kinetic rate of supply provides not only a yearly source of energy, but also the source of solubilized nutrients and environmental conditions for growth. Cell death rates are not included in the model. Therefore, the values calculated by MING represent the maximal biomass that could be sustained based on the kinetic rates of supply. Figure 2 depicts the general flow of a MING calculation.

Through MING's graphical user interface and the use of detached input tables, users are given the opportunity to create unlimited modeling environments. The user may define and use any thermo-hydrological model (temperature and humidity vs. time). The MING model can be run from 2 to 1,000,000 years in any size tunnel (or borehole) with any near-field porosity. The user can define, select, and combine different material sets for both the repository and the waste package as well as gas and water profiles. The user may also select different sets of half reactions and specify the minimum energy necessary for the half reaction to be used as well as the minimum relative humidity and maximum temperature that allow microbial growth. Finally, the user can specify whether gases (N_2, CO_2, and O_2) are included in the model or not. H_2 was not included due to the limited effects of radiolysis.

3.1 Time dependent supply rates

MING is designed to consider all of the committed materials (i.e. those that remain in the drift after permanent closure) that are included in the current repository and waste package (WP) designs (Figure 1), as well as the potential to evaluate any alternate design options that are relevant to microbial behavior. For example, in MING, a committed material (e.g., steel sets, drip shield, etc.) is broken down based on a fractional corrosion rate (1/estimated material lifetime) for that given material. The nutrients and energy made available by degradation are added to the system in a step-wise fashion. These are shown on Table 2. These nutrients also need to be related to the appropriate redox equations that generate the energy needed for growth and metabolism (Table 1). This is done by establishing reactant compositions for each material used in the repository design as shown on Table 3. In addition MING considers time dependent rates on gas supply (Table 4), water composition (Table 5), water flux into the drift (Figure 3), temperature and RH in the drift (Figure 3).

3.2 Corrections to ΔG_r° for pH and temperature

MING considers redox couples to supply the energy required to carry out basic microbiological metabolic functions (i.e., oxidation of electron donors and reduction of electron acceptors). Because organisms tend to utilize specific, well-documented metabolic pathways, a list of appropriate redox half reactions was derived (Table 1) based on the available nutrients in the system that will maximize energy production. MING uses the same values used by

Grogan and McKinley (1990, Appendix 3, p. AIII-1) for the limits of usable energy available from a given full redox reaction, where 15 kJ per mole of electrons transferred is the lower limit of energy required to create biomass (i.e. only those full reactions that produce >15kJ/mol are considered). The final available energy value is converted to microbial mass at a rate of 1 kg of biomass for every 64 MJ of useable energy.

Energy calculations in MING are based on a thermodynamic approach where Gibbs free energies (ΔG) are used to calculate the available energy for microbial production. For example, any redox reaction can be written in the general form

$$A + ae^- + bH^+ = cB + dH_2O \quad (1)$$

for which a standard free energy of reaction (ΔG_r°) can be specified. The ΔG_r° can be derived from standard free energies of formation (ΔG_f°):

$$\Delta G_r^\circ = \sum \Delta G_f^\circ(\text{products}) - \sum \Delta G_f^\circ(\text{reactants}) \quad (2)$$

or from an equilibrium constant (K):

$$\Delta G_r^\circ = -RT \ln K \quad (3)$$

Where R represents the gas constant and T represents the absolute temperature. The calculations are made by combining independent half reactions and calculating the overall ΔG_r° for the reaction.

The temperature of the repository will vary over time (Figure 3). Therefore, a method to incorporate temperature effect on reaction free energies was derived using output calculated using SUPCRT92 (Johnson et al. 1992). Regression analyses were performed on ΔG_r° values at temperatures ranging from 0° to 150°C for a selected group of half reactions to define temperature dependent curves that could be incorporated into the energy calculations. Data selection and regression analyses are documented in Jolley (2001a) with the results shown on Table 1 below. The derived regression variables are used to calculate the temperature dependent ΔG_r° that is used in the derivation of the available energy for a given reaction. The temperature dependent regression variables are used in MING in the following way:

$$\Delta G_{rtemp}^\circ = B_0 + B_1 T + B_2 T^2 \quad (4)$$

where B_0, B_1 and B_2 are the second order regression coefficients. Thus, the effect of variable temperature (°C) are accounted for in the calculations.

In order to account for a chemically variable system, material degradation rates and the time dependent temperatures, gas fluxes, and water chemistries need to be accounted for over the time frame of the calculations. One effect that is directly accounted for is changes to free energy that could be imposed by the pH of incoming water. The free energy is corrected for the pH of the incoming ground water (pH_{H2O}) by applying the following relationship

$$\Delta G_{pH} = \Delta G^{\circ}_{rtemp} - RT \ln[pH_{H2O}] \quad (5)$$

For each full reaction, correcting for the actual pH brings the free energies of reaction further from the standard state values. However, using this simplified model should allow increased understanding of the complexity of the microbiological system and provide a mechanism to evaluate the overall system within an order-of-magnitude.

It is important to note that within MING, only the standard-state free energies are used and these are not corrected for either Eh or the activity of dissolved species to derive the actual nonstandard-state free energies. By not calculating the nonstandard-state free energies, the calculation of available energy is not precise, but only represents a rough estimate of this value. Because the half-reactions are written as simple reduction reactions, the free energy of a full reaction applies more generally than purely standard-state conditions. It is actually constrained such that the ion activity ratios of the redox pairs are at isoactivities, which could be possible for ion activities different than unity (the standard-state conditions). Within a biofilm or an individual organism, the pH (and chemical speciation) can certainly be completely different than the bulk chemistry imposed by the in-drift or near-field environment. However, the bulk chemistry is the major influence on the types of nutrients and energy available for a given organism or biofilm.

3.3 Nutrient supply

As documented in the microbial modeling approach for the Swiss Low/Intermediate-Level Repository (Grogan and McKinley 1990), MING only considers the major elements essential for cell growth (C, N, S, and P). Other nutrients will be considered freely available (i.e., Na, K, Ca, and Cl). The nutritional needs of organisms are handled in MING by using the stoichiometric representation for microbial composition along with other required properties of microorganism as reported in McKinley et al. (1997) and shown in Table 6.

The mass balance calculations conducted in MING consider three sources of nutrient supply: first, the time dependent flux of groundwater into the repository (Table 5 and Figure 3); second, the degradation of repository materials including the multilayered effects (i.e. the waste is not available for nutrient and energy supply until the

waste package is breached; see Section 3.4 below) of waste packages (see Table 2), and third, the time-dependent flux of gases (CO_2, N_2, H_2, and O_2, see Table 4) into the repository. The nutrient limits will be calculated by determining the appropriate ratio (relative molar concentration) of material (determined by available nutrient flux) needed to create the prototypical organism having the stoichiometry in Table 6.

3.4 Other code features

In calculating nutrient availability, MING also will allow a sequential introduction of waste package and ground support materials. This means that a sequential model of a waste package can be defined, where the internal waste package materials are not allowed to mutually degrade and be released into the nutrient stream until the outer shell is completely used up (Table 7).

Another tool that MING utilizes is a special reactant flag where the intermediate breakdown products (other than the basic chemical composition) can be identified. Potential items that fall into this area are substances such as organic admixtures, which are common components of cement mixtures and tend to be resistant to biodegradation. These items can then have their releasable compositional quantities split among associated species included in the redox model (Table 8)

4. Modeling results

4.1 The Swiss low level repository test case

As MING is a new model and comparing results from MING with previously modeled system builds confidence in the model, the Swiss low level repository concept was modeled using the inputs found in Grogan and McKinley (1990), and Capon and Grogan (1991). The results indicate that the portions of the nutrient and energy models used in both the Swiss model and MING are operating in the same way. Figure 5 shows a result comparison for both the energy and nutrient calculations reported by Capon and Grogan (1991) with those calculated with MING. From Figure 5, it can be seen that the results are identical.

4.2 Comparison with laboratory experiments

Experiments conducted at Lawrence Livermore National Laboratory to determine limiting nutrients to microbial growth in the YMP environment and to give bounds on microbial influenced corrosion (MIC) on waste packages are utilized in this model to build confidence. These experiments were conducted independent of model development and are intended to be a blind test on the results of the simulated tests calculated from MING. A description of these results are reported in Horn et al. (1998a and 1998b),Davis et al. (1998), and Horn et al. (2002). These experiments utilize several different growth media. Each of these media was selected to determine the limiting nutrients in the

host rock at YM. Each media was specifically selected to enable the determination of limiting nutrients in the repository environment. The reader is referred to Horn et al. (1998a and 1998b) and Davis et al. (1998) for more detailed descriptions of the experiments.

Each of these media was placed in a flask in addition to a known quantity of Topopah Spring tuff and was cultured for approximately seven days to determine the growth rates and final cell densities. Growth rates were determined by taking samples of the media and periodically subjecting them to live plating; only aerobic heterotrophic organisms were enumerated in these experiments. Two different types of tests were conducted: first, a set of microcosm experiments where the crushed tuff was exposed to a continuous feed of growth media and second, a set of batch experiments where the crushed tuff was exposed to a single aliquot of growth media. The experiments that best fit the setup of MING to model are the batch experiments as they use easily duplicated conditions. Results calculated in MING using the batch experiment inputs are reported on Table 10.

For the six growth media shown in Table 10, the results show on average that MING adequately replicates the lab tests to within 17 percent and are generally accurate to within one order of magnitude. For the phosphate deficient growth media, the results of MING are extremely sensitive to the material lifetime of the tuff. This reflects and supports the conclusion that phosphate is a limiting growth nutrient, as was shown in laboratory experiments. Overall, the results shown in Table 10 reflect the nutrient limiting conditions set up in the lab. By decreasing the material lifetime of the tuff, the MING results will come closer to the measured values. For the carbon deficient media results, there are some concerns. The MING results show a two order of magnitude discrepancy with the values measured in the lab. However, when sensitivity calculations are done on the ΣCO_3 to account for a decrease in ΣCO_3 due to the potential precipitation of calcite or an unknown imposed CO_2 fugacity on the carbon deficient growth media, calculated values approach those measured in the lab experiments.

4.3 Yucca Mountain ambient conditions

Eighteen ambient calculations were done to demonstrate that MING gives a reasonable answer when modeling natural systems. Three separate test case sets were developed, each dependant on the likely nutrient and energy sources: biotite, altered tuff (AT) and unaltered tuff (UT). Each of the three test case sets differed by altering two inputs thought to be the biggest factors to natural microbial variability, water infiltration rate (water availability) and material lifetime of the rock. Two cases were used to look at the variability that infiltration has on the ambient system. In addition to the infiltration rate, the material lifetime for the alteration of the repository host rock seems to be the most uncertain parameter. Because this rate can provide different quantities of nutrients (especially

phosphorous) and energy, this parameter was varied. Figure 6 compares the results provided in the three test cases above with the actual measurements taken at Rainer Mesa and in the Exploratory Studies Facility (ESF) at YM. They show that most calculated results are near or within the measured natural variability and seem reasonable in comparison to the inputs.

Two factors may affect the variability of the results. First there could be some nutrient contamination (not accounted for before sampling) or enhanced growth that allowed the measured ESF and Rainer Mesa tunnel values to be elevated because the sampling took place well after the tunnels were constructed (Kieft et al. 1993, Haldeman and Amy 1993). Second, our model is abstracted, and therefore we may not have included a measurable quantity of an energy-providing nutrient. Even with the above factors in mind, the ambient case results seem to indicate that we are modeling the ambient system adequately. The results also indicate the dependence of microbial growth on groundwater composition and flux, especially since the ESF experiments indicate that water is the limiting nutrient in the ambient system (Kieft et al. 1997, Horn et al., 2002). To some extent, the modeling results also indicate that the composition and material lifetime of the altered and unaltered tuff can play a role in the abundance of microorganisms, however the solubilization of rock is also affected by microbial activity (Horn et al., 2002). Phosphorous is less abundant in the unaltered tuff and its availability is generally limited to the concentrations found in the tuff.

4.4 Modeling the engineered barrier system (EBS) at Yucca Mountain

The case presented below represents a modeling scenario that uses the specific inputs presented above. The case presented is a representative case for the current EBS design shown on Figure 1. Other representative cases are reported in Jolley (2000). Results shown on Figure 4 indicate that the maximum yearly biomass produced for the entire calculation is 55.54 g_{dry}/m of drift in year 363,636. During the ventilation period prior to repository closure (0 to 51 years) the biomass production was between 15.21 and 14.36 g_{dry}/m of drift during times when the T and RH were below the threshold for growth. Otherwise, no growth occurred until well into the post closure period (in year 324) due to elevated temperatures or low RH. Maximum biomass growth attributable to degradation of ground support of 4.10 g_{dry}/m occurred in year 780 due to the degradation of the steel in the gantry rails. The biomass decreases to 0.19 g_{dry}/m of drift when the final ground support component (cement grout comprised of Type K cement, silica fume and superplasticizer) degraded in year 2,500. Later, the drip shield produced a maximum of 0.0549 g_{dry}/m at year 150,000 and the natural ambient system produced a biomass of 0.0542 g_{dry}/m after the waste form was degraded in year 364,735. After the drip shield fails the waste package and pallet produce a maximum

biomass of 11.09 g_{dry}/m during degradation of the stainless steel in the waste package pallet (pedestal) and a biomass of 0.11 g_{dry}/m for the C-22 alloy materials (waste package outer shell and pedestal). Biomass production during the waste form degradation period (363,636 to 364,735) was at its peak (55.54 g_{dry}/m) due to the rapid degradation of the waste package inner shell and the basket materials. For the majority of the lifetime of the waste form, the biomass produced ranged between 55 and 11 g_{dry}/m.

During most of the period covered by the calculation, biomass growth in the repository environment is nutrient limited by the lack of phosphorous in the groundwater fluxing into the repository (Table 9). Prior to year 324, the biomass is limited because the RH was too low or the temperature too high to sustain microbial growth. The only time that the calculation is energy limited is during the preclosure ventilation period. During times when the repository is limited by carbon, it is because there is not enough available in the materials being degraded in the repository and the energy utilization of CO_2 gas is small. Over the one million-year calculation of the EBS, a cumulative biomass of 1.98E+06 grams per meter of drift is produced.

5. Conclusions

With the advent of MING, a forward predictive capability of the effects of microbiological communities can be explored. Several predictive capabilities are currently possible using results of this model. These capabilities include determination of biofilm production, CO_2 gas production, radionuclide sorption, microbial colloid formation and siderophore production. These types of predictive models are important not only to the Yucca Mountain project and to its potential mission as a nuclear waste repository, but to other investigations and projects that deal with future and past interactions between geologic or engineered materials and the biosphere. The model as presented above does not address all of the specific effects of the localized impacts of biofilm development, colloid formation, and the production of inorganic acids, methane, organic byproducts, carbon dioxide, and other chemical species that could change the longevity of materials. However, the results from MING have been used to establish bounds on CO_2 production, biofilm formation, generation of colloids and uptake of radionuclides by microorganisms in in-drift environments (Jolley, 2000 and Jolley 2001b). Examples for CO_2 gas estimation and radionuclide transport are discussed below.

5.1 CO_2 gas respiration estimation

The generation of CO_2 gas was one of the first predictive uses of MING modeling. CO_2 gas availability is important in the solubility of radionuclides such as Uranium and Neptunium. The prediction is based on the methodology

discussed in Morel and Hering (1993, Chapter 4 Section 7.1) where the protoplasm term for a chemical reaction is equated to the major elements in an algal biomass and the respiratory process is defined by the following reactions:

$$\text{Protoplasm} = C_{106}H_{263}O_{110}N_{16}P_1 \quad (6)$$

$$\text{Protoplasm} + 138O_2 \Rightarrow 106CO_2 + 16NO_3^- + H_2PO_4^- + 122H_2O + 17H^+ \quad (7)$$

Therefore, if we equate our microbial stoichiometric formula [$C_{160}(H_{280}O_{80})N_{30}P_2S$; Table 6] to the protoplasm term, we can then determine an estimate of the number of moles of CO_2 that could be generated by a given number of moles of heterotrophic organisms.

$$C_{160}(H_{280}O_{80})N_{30}P_2S + 209O_2 \Rightarrow 160CO_2 + 80H_2O + 30NO_3^- + 2H_2PO_4^- + H_2S + 114H^+ \quad (8)$$

Thus, a maximum of 160 moles of CO_2 could be produced for every mole of microorganisms that would respire. Figure 7 below was generated by taking the mass of organisms from several modeling cases discussed in Jolley (2000; Note that Case 1 is very similar to Case 2 shown on Figure 4), and calculating the moles of CO_2 per cubic meter of drift. Notice that one can also use this equation to determine O_2 consumption as well.

5.2 Radionuclide Sorption

Results from Jolley (2001b) indicate that there is a large potential in the repository drift for radionuclides to sorb onto microorganisms, with the possibility that adsorbed nuclides could subsequently transport with organisms in groundwater effluxed from the repository drifts. Figure 8 uses cumulative results from MING calculations in Jolley (2000) like those shown on Figure 4 to derive a time dependent microbial source term in the drift. This source term coupled with a distribution of uranium uptake allows for the predictive modeling of the effects of microbial sorption and subsequent modeling of colloidal transport. The distribution is derived from experimental results of sorption on microorganisms due to metabolism-independent uptake onto cell walls and membrane components. Uptake averages 162.88 ± 133.05 mg/gm dry cell weight and range from a minimum value of 45.2 mg/g to a maximum of 615 mg/g. These data were derived from Suzuki and Banfield (1999).

Figure 8 shows that the distribution in the mass of uranium that can be accumulated on the predicted biomass over 1 million years. Therefore, over a period of 1 million years, the biomass produced in the EBS can uptake from 178 to 2423 kg of uranium for one meter of drift containing a commercial spent nuclear fuel waste package as long as the pH of the environment stays acidic or near neutral. The fate of the resulting colloids with respect to their transport by groundwater remains to be determined by further studies.

5.3 Other potential uses

Although no modeling results have been provided, we believe that MING can be adapted to evaluate other types of environmental problems. Theoretically, any investigation of a natural system that involved the determination of *in-situ* microbial communities could be modeled. As an example, Figure 9 depicts the spatial set up of a typical repository drift-based calculation. The flux of items such as groundwater and gas are downward in the horizontal direction. However, if the same figure were rotated 90°, it would depict a standard borehole. Therefore, any investigation that could be conducted within a borehole could be examined.

MING could be especially useful in the investigation of monitored natural attenuation and engineered bioremediation projects to clean up contaminated subsurface locations. In addition to the predictive tools generated for use on the Yucca Mountain Project, the investigation of site remediation issues concerning geochemistry and transport discussed above, like CO_2 gas generation and radionuclide sorption, other potential uses are numerous. Examples include the determination or quantification of the biomass possible from the addition of fertilizers in planned *in-situ* remediation projects. The optimization of alternative bioremediation designs can be investigated. Predictions on non-radionuclide sorption and generation of CO_2 gas in landfills or other waste locations can be made. Of course, the use of MING is not limited to these few examples.

Acknowledgments

This work was supported by the U.S. DOE Yucca Mountain Site Characterization Office under contract # DE-AC08-01NV12101 to Bechtel SAIC Company LLC. The authors would like to thank David Sassani, Pat O'Connell, Paul Domski, James Schreiber, Annemarie Meike, and Simcha Stross-Gasgoyne for their assistance in conceptual model development and the development and testing of the software. Thanks also go to Amy Loch, Patrick Brady, and Larry Hersman for their reviews of the manuscript.

References

Amy, P.S. 1997. Microbial Dormancy and Survival in the Subsurface. Chapter 11 of The Microbiology of the Terrestrial Deep Subsurface. Amy, P.S. and Haldeman, D.L., eds. CRC Lewis Publishers. p. 185-204.

Amy, P.S. and Haldeman, D.L. 1997. The Microbiology of the Terrestrial Deep Subsurface. CRC Lewis Publishers. 356 p.

Bachofen, R. 1991. Gas Metabolism of Microorganisms. Experientia, 47, pp. 508-513.

Banfield, J.F. and Nealson, K.H., eds. 1997. Geomicrobiology: Interactions Between Microbes and Minerals. Reviews in Mineralogy Volume 35. Mineralogical Society of America. 448 p.

Brown, A.D. 1976. Microbial Water Stress. Bacteriological Reviews, 40 (4), 8703-846.

Capon, P. and Grogan, H. 1991. EMMA, A User Guide and Description of the Program. IM2661-2. Nationale Genossenschaft fur die Lagerung radioaktiver Abfalle. 42 p.

Davis, M.A.; Martin, S.; Miranda, A.; and Horn, J.M. 1998. Sustaining Native Microbial Growth with Endogenous Nutrients at Yucca Mountain. URCL-JC-129185. Lawrence Livermore National Laboratory. 6 p.

Ehrhorn, T.F. and Jolley D.M. 1998a. Life Cycle Plan, MING Microbial Impacks to the Near-Field Environment Geochemistry Version 1.0 CSCI 30018 V1.0. CSCI: 30018 V1.0. DI: 30018-2001 Rev 0. Las Vegas, Nevada: CRWMS M&O. 15p.

Ehrhorn, T.F. and Jolley D.M. 1998b. Computer Software Documentation and Users Manual, MING Microbial Impacts to the Near-Field Environment Geochemistry Version 1.0 CSCI 30018 V1.0. CSCI: 30018 V1.0. DI: 30018-2003, Rev. 0. Las Vegas, Nevada: CRWMS M&O. 90 p.

Grogan, H.A. and McKinley, I.G. 1990. An Approach to Microbiological Modeling: Application to the Near Field of a Swiss Low/Intermediate-Level Waste Repository. Technical Report 89-06. Nationale Genossenschaft fur die Lagerung radioaktiver Abfalle. 29 p.

Haldeman, D.L. and Amy, P.S. 1993. Bacterial Heterogeneity in Deep Subsurface Tunnels at Rainier Mesa, Nevada Test Site. Microbial Ecology, 25, (2), 185-194.

Hersman, L.E. 1997. Subsurface Microbiology: Effects on the Transport of Radioactive Wastes in the Vadose Zone. Chapter 16 of The Microbiology of the Terrestrial Deep Subsurface. Amy, P.S. and Haldeman, D.L., eds. CRC Lewis Publishers. pp. 299-324.

Horn, J.M. and Meike, A. 1995. Microbial Activity at Yucca Mountain. Part I: Microbial Metabolism, Adaptation and the Repository Environment. UCRL-ID-122256. Lawrence Livermore National Laboratory. 54 p.

Horn, J.M.; Davis, M.; Martin, S.; Lian, T.; and Jones, D. 1998a. Assessing Microbiologically Induced Corrosion of Waste Package Materials in the Yucca Mountain Repository. URCL-JC-130567. Lawrence Livermore National Laboratory. 18 p.

Horn, J.M.; Rivera, A.; Lian, T.; and Jones, D. 1998b. MIC Evaluation and Testing for the Yucca Mountain Repository. Proceedings of Corrosion 98, March 22-27, NACE International. pp. 152/2 to 152/14.

Horn, J. M. and Jones, D. 2002. Microbiologically Influenced Corrosion: Perspectives and Approaches. Section 97 in Manual of Environmental Microbiology, second edition, C.J. Hurst, R.L. Crawford, G.R. Knudsen, M.J. McInerney, and L.D. Stetzenbach, eds., American Society of Microbiology Press, p. 1072-1083.

Horn, J.M., Masterson, B.A., Rivera, A., Miranda, A., Davis, M.A. and Martin, S. 2002. Bacterial Growth Dynamics, Limiting Factors, and Community Diversity in a Proposed Geological Nuclear Waste Repository Environment. Geomicrobiology, in press.

Johnson, J. W., Olkers E. H., and Helgeson H. C., 1992. SUPCRT92: A Software Package for Calculating the Standard Molal Thermodynamic Properties of Minerals, Gases, Aqueous Species and Reactions from 1 to 500 Bar and 0 to 1000C. Computers and Geosciences 18 (7), pp. 899-247.

Jolley, D. M. 2000. In-Drift Microbial Communities, ANL-EBS-MD-000038 Rev 00 ICN 01. Las Vegas, Nevada: CRWMS M&O. 174 p.

Jolley, D. M. 2001a. Microbial Communities Model Parameter Calculations for TSPA/SR, CAL-EBS-PA-000001 Rev 00. Las Vegas, Nevada: BSC (Bechtel SAIC Company). 37 p.

Jolley, D. M. 2001b. Microbial Transport Sensitivity Calculations, CAL-EBS-PA-000011 Rev 00 ICN 01. Las Vegas, Nevada: BSC (Bechtel SAIC Company). 23 p.

Jolley, D. M. 2001c. In-Drift Microbial Communities Model Validation Calculations, CAL-EBS-EV-000001 Rev 00 ICN 02. Las Vegas, Nevada: BSC (Bechtel SAIC Company). 50 p.

Kieft, T.L. and Phelps, T.J 1997. Life in the Slow Lane: Activities of Microorganisms in the Subsurface. Chapter 9 of The Microbiology of the Terrestrial Deep Subsurface. Amy, P.S. and Haldeman, D.L., eds. Lewis Publishers. pp. 137-164.

Kieft, T.L.; Amy, P.S.; Brockman, F.J.; Fredrickson, J.K.; Bjornstad, B.N.; and Rosacker, L.L. 1993. Microbial Abundance and Activities in Relation to Water Potential in the Vadose Zones of Arid and Semiarid Sites. Microbial Ecology, 26, pp. 59-78.

Kieft, T.L.; Kovacik, W.P., Jr.; Ringelberg, D.B.; White, D.C.; Haldeman, D.L.; Amy, P.S.; and Hersman, L.E. 1997. Factors Limiting Microbial Growth and Activity at a Proposed High-Level Nuclear Repository, Yucca Mountain, Nevada. Applied and Environmental Microbiology, 63, (8), pp. 3128-3133.

Little, B.J.; Wagner, P.A.; and Lewandowski, Z. 1997. Spatial Relationships Between Bacteria and Mineral Surfaces. Geomicrobiology: Interactions Between Microbes and Minerals. Banfield, J.F. and Nealson, K.H., eds. Reviews in Mineralogy Volume 35, pp. 123-159.

Lovley, D.R. and Phillips, E.J.P. 1992. Reduction of Uranium by Desulfovibrio Desulfuricans. Applied and Environmental Microbiology, 58, (3), pp. 850-856.

Lovley, D.R.; Phillips, E.J.P.; Gorby, Y. A.; and Land, E.R. 1991. Microbial Reduction of Uranium. Nature, 350, (6317), pp. 414-416.

Lovley, D.R.; Widman, P.K.; Woodward, J.C.; and Phillips, E.J.P. 1993. Reduction of Uranium by Cytochrome c3 of Desulfovibrio Vulgaris. Applied and Environmental Microbiology, 59, (11), pp. 3572-3576.

McKinley, I.G. and Grogan, H.A. 1991. Consideration of Microbiology in Modeling the Near Field of a L/ILW Repository. Experientia, 47, pp. 573-577.

McKinley, I.G.; Hagenlocher, I.; Alexander, W.R.; and Schwyn, B. 1997. Microbiology in Nuclear Waste Disposal: Interfaces and Reaction Fronts. FEMS Microbiology Reviews, 20, (3-4), pp. 545-556.

Morel, F.M.M. and Herring J.G. 1993. Principles and Applications of Aquatic Chemistry, John Wiley and Sons, 588 p.

Morita, R.Y. 1990. The Starvation-Survival State of Microorganisms in Nature and Its Relationship to the Bioavailable Energy. Experientia, 46, pp. 813-817.

O'Connell, P.A. 1998. Software Qualification Report MING Microbial Impacts to the Near-Field Environment Geochemistry Version 1.0. CSCI: 30018 V1.0 . DI: 30018-2003, Rev. 00. Las Vegas, Nevada: CRWMS M&O. 58 p.

Pedersen, K. and Karlsson, F. 1995. Investigations of Subterranean Microorganisms: Their Importance for Performance Assessment of Radioactive Waste Disposal. SKB 95-10. Swedish Nuclear Fuel and Waste Management Company. 222 p.

Stroes-Gascoyne, S. 1989. The Potential for Microbial Life in a Canadian High-Level Nuclear Fuel Waste Disposal Vault: A Nutrient and Energy Source Analysis. AECL-9574. Atomic Energy of Canada Limited. 59 p.

Suzuki, Y. and Banfield, J. F. 1999. Geomicrobiology of Uranium, in Uranium: Mineralogy, Geochemistry and the Environment Geomicrobiology: Burns P.C. and Finch R., eds. Reviews in Mineralogy Volume 38, pp. 393-432.

FIGURE CAPTIONS

Figure 1. Components of the Engineered Barrier System in the Proposed Repository at Yucca Mountain

Figure 2. Schematic Diagram Showing the Inputs and Functionality of MING

Figure 3. Waste Package Temperatures and Relative Humidities and Percolation Flux at the Repository Drift Wall through Time used in MING Calculations (Jolley 2000)

Figure 4. Biomass Production through Time for One Meter of Drift Containing a 21 PWR Waste Package (Jolley 2000)

Figure 5. Comparison of Swiss Model Results (Capon and Grogan, 1991) with MING Calculations of the Swiss Model (Jolley 2000)

Figure 6. Comparison of MING Results to Ambient Measurements. The Dashed Lines Represent the Ranges in Measured Data in The ESF and The Rainier Mesa Analog on the Nevada Test Site. Results Represent Two Different Groundwater Infiltration Rates (Cases 1-3 use 7.8 Mm/Yr And Cases 4-6 use 42.06 Mm/Yr) and Three Different Lithologic Compositions of Topopah Spring Tuff (Biotite Only, Unaltered Tuff [UT] and Altered Tuff [AT]) (Jolley 2001c).

Figure 7. Estimating CO_2 Gas Generation via Microbial Respiration Using MING Modeling Results (Jolley 2000) Results of Case 1 are Similar to Results Shown in Figure 4. Case 7 Represents Maximum Corrosion of In-drift Ground Support Components, Case 15 and 21 Represent the Same Input as Case 1 and 7 Respectively with the Substitution of the PWR Commercial Spent Fuel Waste Package with the High Level Waste Glass Waste Packages. The Final Case Represents Case 1 Modeled with a 44 BWR Waste Package.

Figure 8. Uranium Uptake onto Biomass Generated from a Microbial Source Term Representing Commercial Spent Nuclear Fuel Waste Packages in a Potential Repository Drift.

Figure 9. Configuration of a Repository Drift Model vs. a Borehole Model. Note that MING is set up to handle cylindrical volumes and fluxes directed perpendicular to the cylinder.

TABLES

Table 1. ΔG (kJ/mol) as a Function of Temperature (°C) for Selected Redox Half Reactions (Jolley 2001a).

Redox Half Reactions	$\Delta°G_r = B_0 + B_1T + B_2T^2$			Redox Half Reactions	$\Delta°G_r = B_0 + B_1T + B_2T^2$		
	B_0	B_1	B_2		B_0	B_1	B_2
$CO_2 + H^+ + 2e^- = HCOO^-$	40.7454	0.1077	1.6658e-4	$NO_3^- + 9H^+ + 8e^- = NH_3 + 3H_2O$	-623.0305	-0.1508	-4.9350e-4
$CO_2 + 4H^+ + 4e^- = CH_2O + H_2O$	-35.1181	0.0353	4.8168e-4	$Fe_2O_3 + 6H^+ + 6e^- = 2Fe + 3H_2O$	38.2658	-0.1731	-1.9358e-4
$CO_2 + 6H^+ + 6e^- = CH_3OH + H_2O$	-19.0661	0.0166	-2.5150e-4	$Fe^{2+} + 2e^- = Fe$	94.6318	-0.1220	-1.1699e-4
$HCOO^- + 3H^+ + 2e^- = CH_2O + H_2O$	6.3612	-0.0736	-3.4507e-4	$Fe^{3+} + e^- = Fe^{2+}$	-70.1995	-0.1605	-1.0569e-4
$CO_2 + 8H^+ + 8e^- = CH_4 + 2H_2O$	-114.3373	-0.0056	-4.0214e-4	$Fe_3O_4 + 8H^+ + 8e^- = 3Fe + 4H_2O$	71.5929	-0.2109	-2.5541e-4
$CH_2O + 2H^+ + 2e^- = CH_3OH$	-66.1411	-0.0175	-7.3149e-5	$FeOOH + 3H^+ + e^- = Fe^{2+} + 2H_2O$	-77.7134	0.0139	3.2389e-5
$HCOO^- + 7H^+ + 6e^- = CH_4 + 2H_2O$	-154.9582	-0.1142	-5.6428e-4	$MnO_2 + 4H^+ + 2e^- = Mn^{2+} + 2H_2O$	-239.0315	-0.0302	-2.5681e-5
$CH_2O + 4H^+ + 4e^- = CH_4 + H_2O$	-161.3965	-0.0339	-2.4447e-4	$Mn_3O_4 + 8H^+ + 2e^- = 3Mn^{2+} + 4H_2O$	-359.3919	0.0602	2.9471e-5
$CH_3OH + 2H^+ + 2e^- = CH_4 + H_2O$	-95.1077	-0.0244	-1.4081e-4	$S + H^+ + 2e^- = HS^-$	13.2571	-0.0571	2.3278e-4
$CO_3^{2-} + 10H^+ + 8e^- = CH_4 + 3H_2O$	-210.2704	-0.2960	-1.0161e-3	$S + 2H^+ + 2e^- = H_2S$	-25.6245	-0.0922	1.3593e-4
$CO_3^{2-} + 6H^+ + 4e^- = CH_2O + 2H_2O$	-48.9273	-0.2572	-7.9106e-4	$SO_4^{-2} + 9H^+ + 8e^- = HS^- + 4H_2O$	-182.7211	-0.2997	-5.9307e-4
$CO_3^{2-} + 8H^+ + 6e^- = CH_3OH + 2H_2O$	-115.0967	-0.2746	-8.6484e-4	$SO_4^{-2} + 10H^+ + 8e^- = H_2S + 4H_2O$	-223.0548	-0.3393	-9.7424e-4
$CO_3^{2-} + 3H^+ + 2e^- = HCOO^- + H_2O$	-55.2133	-0.1845	-4.4713e-4	$HSO_4^- + 7H^+ + 6e^- = S + 4H_2O$	-188.9704	-0.1559	-4.8888e-4
$N_2 + 6H^+ + 6e^- = 2NH_3$	-52.8196	-0.0194	-1.6830e-4	$SO_4^{-2} + 8H^+ + 6e^- = S + 4H_2O$	-197.8705	-0.2466	-8.3085e-4
$N_2 + 8H^+ + 6e^- = 2NH_4^+$	-157.8665	-0.0357	-8.4085e-5	$SO_2 + 4e^- + 4H^+ = S + 2H_2O$	-172.9306	-0.0109	-2.0250e-4
$NO_2^- + 7H^+ + 6e^- = NH_3 + 2H_2O$	-466.1398	-0.1037	-4.3778e-4	$SO_3^{2-} + 7H^+ + 6e^- = HS^- + 3H_2O$	-206.0158	-0.2744	-5.7195e-4
$NO_3^- + 2H^+ + 2e^- = NO_2^- + H_2O$	-156.8907	-0.0470	-5.5727e-5	$2SO_4^{-2} + 10H^+ + 8e^- = S_2O_3^{-2} + 5H_2O$	-211.1992	-0.3248	-9.2009e-4
$NO_3^- + 10H^+ + 8e^- = NH_4^+ + 3H_2O$	-675.9929	-0.1544	-4.6004e-4	$H^+ + e^- = 0.5H_2$	9.5513	-0.0265	-8.8270e-5
$NO_2^- + 8H^+ + 6e^- = NH_4^+ + 2H_2O$	-754.0787	-0.1760	-4.9901e-4	$O_2 + 4H^+ + 4e^- = 2H_2O$	-490.0311	-0.0378	8.0135e-5
$NO_3^- + 6H^+ + 5e^- = 0.5N_2 + 3H_2O$	-597.2461	-0.1342	-4.2457e-4	$UO_2^{2+} + 4H^+ + 2e^- = U^{4+} + 2H_2O$	-55.8741	0.1679	-5.1626e-5
$2NO_2^- + 8H^+ + 6e^- = N_2 + 4H_2O$	-878.9891	-0.1898	-7.0731e-4				

Selection of data and documentation of regression analyses found in Jolley (2001a)

Table 2. Material Compositions, Masses and Estimated Material Lifetimes for Materials used in the Engineered Barrier System Design (Jolley 2000a)

Materials Used in the Engineered Barrier System Design	Chemical Composition	Mass (Kg/M)	Estimated Material Lifetime (yr)
Steel Sets And Invert	$Fe_{97.48}C_{0.23}P_{0.04}S_{0.05}Si_{0.4}Mn_{1.65}V_{0.15}$	597.25	250
Rock Bolts	$Fe_{99.022}C_{0.79}P_{0.058}S_{0.13}$	48	299
Gantry Rails	$Fe_{97.59}C_{0.82}P_{0.04}S_{0.5}Si_{0.5}Mn_{1.0}$	133.9	782
Welded Wire Fabric	$Fe_{98.8}C_{1.0}P_{0.1}S_{0.1}$	70	52
Type K Cement	$Ca_{44.21}Si_{9.05}O_{36.34}Al_{2.75}Fe_{1.96}S_{2.76}K_{0.49}Na_{0.07}Mg_{0.84}Sr_{0.04}Zn_{0.02}Ti_{0.17}Mn_{0.02}P_{0.04}$	63.5	2500
Silica Fume	$Ca_{0.214}Si_{44.333}O_{51.86}Al_{0.371}Fe_{0.21}S_{0.32}K_{0.249}Na_{0.223}Mg_{0.12}C_{1.30}$	3.35	2500
Superplasticizer	$C_{16.12}H_{8.03}S_{4.28}O_{66.17}Cl_{0.04}Ca_{5.36}$	0.67	2500
Communications Cable	$Cu_{50.0}C_{42.82}H_{7.18}$	0.79	100
Outer Waste Package Shell*	$Mo_{14.5}Cr_{22.5}Fe_{6.0}W_{3.5}Co_{2.5}C_{0.015}Si_{0.08}Mn_{0.50}V_{0.35}P_{0.02}S_{0.02}Ni_{50.015}$	1633	181818
Inner Waste Package Shell	$Fe_{61.795}Mn_{2.0}Si_{1.0}P_{0.045}S_{0.03}Cr_{18.00}N_{0.10}Mo_{3.00}Ni_{14.00}C_{0.03}$	2178	1099
Waste Package Basket Materials	$Fe_{97.91}C_{0.27}P_{0.035}S_{0.035}Ni_{13.00}Mn_{1.3}$	1108	105
Waste Package Neutron Absorber	$Fe_{66.66}C_{0.04}Cr_{18.5}Co_{0.20}B_{1.6}Ni_{13.0}$	400	17.5
Waste Package Thermal Shunt	$Al_{96.00}Si_{0.8}Fe_{0.7}Cu_{0.4}Mn_{0.15}Mg_{1.2}Cr_{0.35}Zn_{0.25}Ti_{0.15}$	65	11.8
Waste Package Pallet	$Fe_{61.805}Mn_{2.0}Si_{1.0}P_{0.045}S_{0.03}Cr_{18.00}N_{0.10}Mo_{3.00}Ni_{14.00}C_{0.02}$	165	209
Drip Sheld	$Ti_{99.055}N_{0.03}C_{0.1}H_{0.015}O_{0.25}Fe_{0.3}Pd_{0.25}$	670	57692
Spent Nuclear Fuel**	$Fe_{1.85}P_{0.01}Mn_{0.05}C_{0.01}N_{0.01}$	3145	500

Note: The inputs listed here represent a one meter repository drift segment that is located in the Topopah Spring middle nonlithophysal unit containing a 21 PWR waste package. Material lifetimes represent are representative of rapid corrosion rates as documented in Jolley (2000). Use of other representative material lifetimes drift locations, waste package types and waste forms and their modeling results can be found in Jolley (2000).

* Alloy 22; the mass includes part of the same material used in the waste package pallet (343 kg/m).

** The composition only includes the elements used in MING nutrient and redox equations. Uranium was not included in this set of calculations as an electron acceptor.

Table 3. Reactant Compositions Used in the Energy Calculations for Each Material in the Engineered Barrier System Designs (Jolley 2000).

EBS Material	Reactant Compositions
Waste Package Thermal Shunt	Fe, Mn^{2+}
Steel Sets and Invert	Fe, Mn^{2+}, S, CH_2O
Gantry Rails	Fe, Mn^{2+}, S, CH_2O
Rock Bolts	Fe, S, CH_2O
Waste Package Pallet	CH_2O, Fe, Mn^{2+}, NO_3^-, S
Inner Waste Package Shell	CH_2O, Fe, Mn^{2+}, NO_3^-, S
Waste Package Basket Materials	CH_2O, Fe, Mn^{2+}, S
Waste Package Neutron Absorber	CH_2O, Fe,
Outer Waste Package Shell	Fe, Mn^{2+}, S, CH_2O
Type K Cement	Fe^{2+}, SO_4^{2-},
Gantry Rail	CH_2O, Fe, S, Mn^{2+}
Rail Fittings	CH_2O, Fe, S
Drip Shield	NO_3^-, CH_2O, Fe
Superplasticizer	$HCOO^-$, CH_3OH, CH_2O, SO_3^{2-}
Communications Cable	CH_3OH
Welded Wire Fabric	CH_2O, Fe, S
Silica Fume	Fe^{2+}, SO_4^{2-}, CH_2O
Spent Nuclear Fuel	Fe, NO_3^-, CO_3^{2-}, S, Mn^{2+}

Table 4. Cumulative Gas Flux Values (kg/m^2) into the drift used in MING Calculations (Jolley 2000)

Year	CO_2	O_2	N_2
1	6.6667E-06	9.2800E-04	3.7000E-03
3700	2.4667E-02	3.4336E+00	1.3690E+01
3701	2.4687E-02	3.4382E+00	1.3709E+01
10000	1.5069E-01	3.2670E+01	1.3026E+02
100000	1.9507E+00	4.5027E+02	1.7953E+03
1000000	1.9951E+01	4.6263E+03	1.8445E+04

Table 5. Calculated Drift Wall Water Compositions used in MING (Jolley 2000).

Parameter Time	Preclosure Period	Boiling Period	Transitional Cool-Down Period	Extended Cool-Down Period*
Time	0 - 50 years	50 - 1000 years	1000 – 2000 years	2000 - 100,000 years
pH	8.2	8.1	7.8	7.3
PO_4^{-3} kmol/m^3	1.79E-07	1.79E-07	1.79E-07	1.79E-07
NO_3^- kmol/m^3	1.28E-05	1.28E-05	1.28E-05	1.28E-05
DOC kmol/m^3	3.30E-05	3.30E-05	3.30E-05	3.30E-05
Mn^{2+} kmol/m^3	1.04E-07	1.04E-07	1.04E-07	1.04E-07
CO_3^{2-} kmol/m^3	1.3E-03	1.9E-04	3.0E-04	2.1E-03
SO_4^{-2} kmol/m^3	1.3E-03	6.6E-04	1.2E-03	1.2E-03
Fe^{2+} kmol/m^3	1.1E-10	7.9E-10	4.1E-10	2.4E-11

*These values are used beyond 100,000 years.

Table 6. Stociometric Representation for Microbial Composition along with Other Required Properties of a Microorganism Taken from McKinley et al. (1997)

Microbial Composition	$C_{160}(H_{280}O_{80})N_{30}P_2S$
Average Water Content	99% by weight
Average Microbial Volume	1.5×10^{-13} ml

Table 7. Material Layer Designators Used in MING for the Sequential Degradation of Waste Package and Repository Materials (Jolley 2000).

Material Name	Layer	Material Name	Layer	Material Name	Layer
WP Pallet	2	Gantry Rail	0	Superplasticizer	0
WP Inner Shell	3	Rock Bolts	0	Ti Grade 7	1
WP Outer Shell	2	Communications Cable	0	Type K Cement	0
Thermal Shunt	3	WP Neutron Absorber	3	Welded Wire Fabric Steel	0
Steel Sets/Invert	0	Silica Fume	0	WP Basket Materials	3

Table 8. Reactant Compositions, Breakdown Codes and Molecular Masses for the Release of Organic Materials (Jolley 2000).

Reactant Composition	Breakdown Code	Molecular Mass
Superplasticizer		
CH_2O	5	278
CH_3OH	4	
$HCOO^-$	2	
SO_3^{2-}	1	
Communications Cable		
CH_2O	2	28

Table 9. Limiting Environmental Conditions Reported in MING Output (Jolley 2000).

Start Year	Stop Year	Limiting Condition
1	9	Energy Limited
10	24	Humidity Too Low
25	51	Energy Limited
52	323	Humidity Too Low
324	782	Carbon
783	181817	Phosphorus
181818	182026	Carbon
182027	363635	Phosphorus
363636	364734	Carbon
364735	1000000	Phosphorus

Table 10 Comparison of Calculated Results from MING to Laboratory Experiments for Six Different Growth Media (GM) (Jolley 2001c).

Growth Media (GM)	Microorganisms Calculated in MING (per ml GM)	Maximum Microbes in Batch Tests (per mil of GM)	Maximum Microbes in Microcosm Tests (per mil of GM)	Difference Log10[MING] - Log10[batch])	Difference Log10[MING] - Log10[microcosm])
YM complete	1.04E+08	8.00E+08	7.70E+07	-0.88	0.13
Dilute Complete	2.89E+07	3.80E+06	3.43E+08	0.88	-1.07
J13-NO3	2.03E+08	1.12E+08	4.90E+08	0.26	-0.38
Phosphate Deficient	1.47E+05	4.50E+05	1.10E+07	-0.49	-1.87
J13-SO4	2.03E+08	3.85E+09	7.60E+08	-1.28	-0.57
Carbon Deficient	8.34E+07	1.02E+06	3.60E+06	1.91	1.36
				Average :	-0.17 ± 1.12

FIGURES

Figure 1

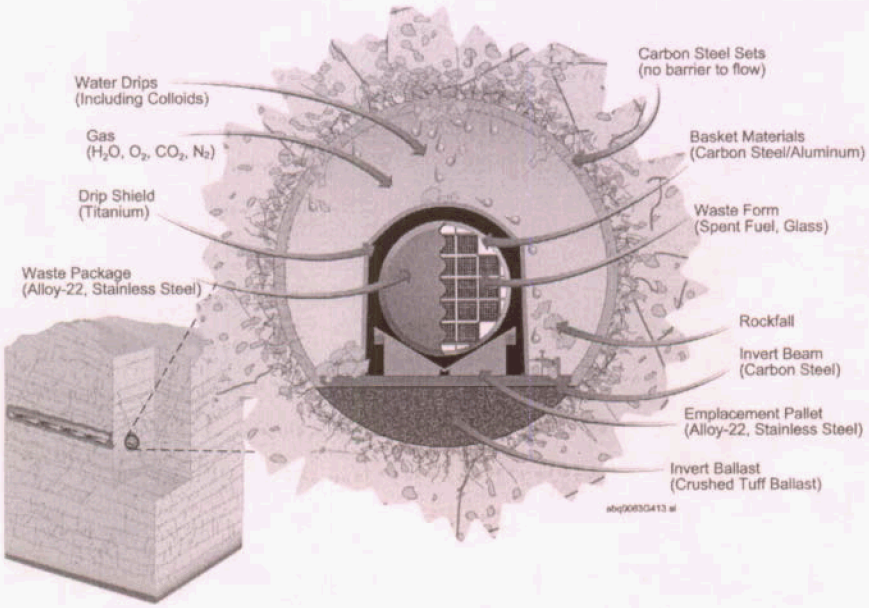

Figure 2

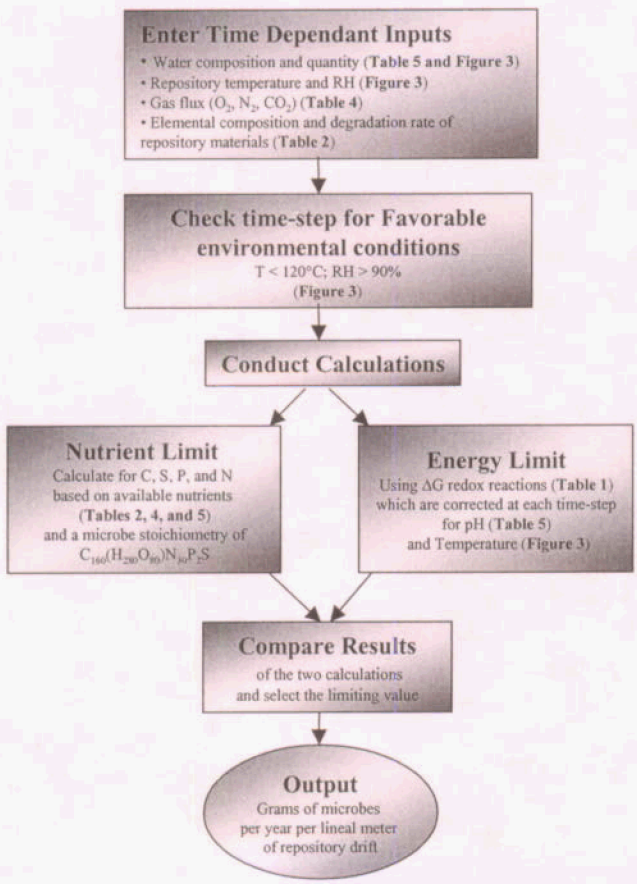

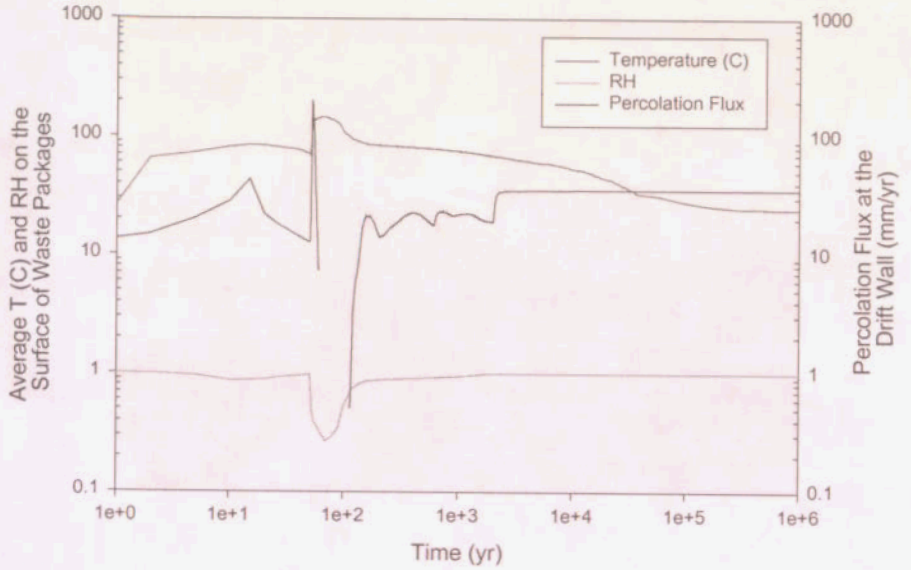

Figure 3

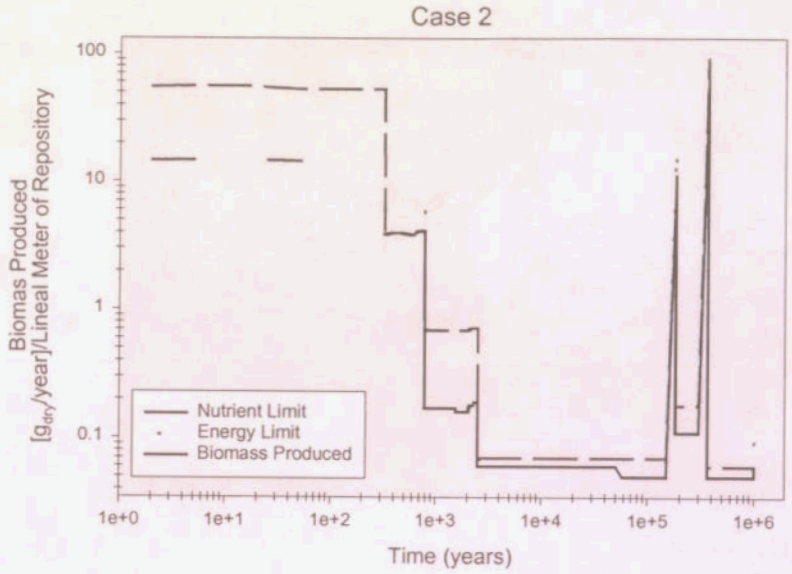

Figure 4

Figure 5

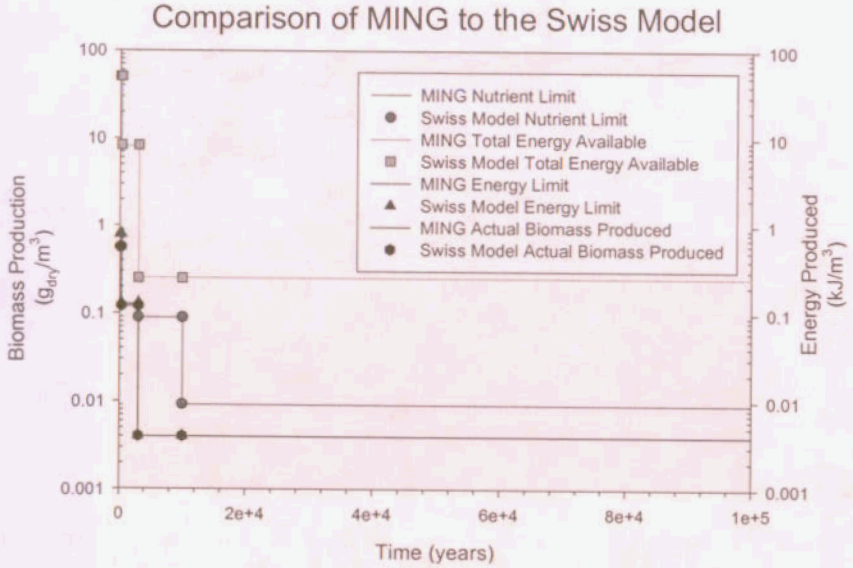

Figure 6

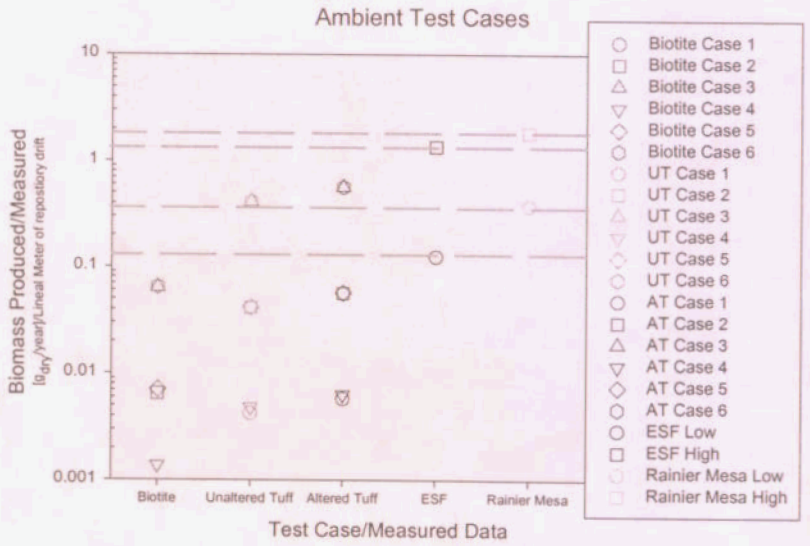

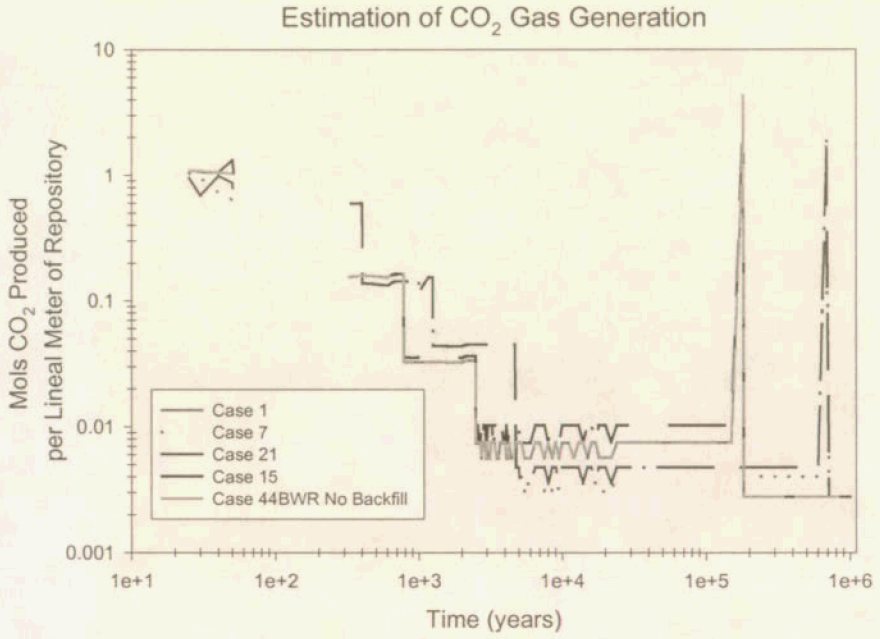

Figure 7

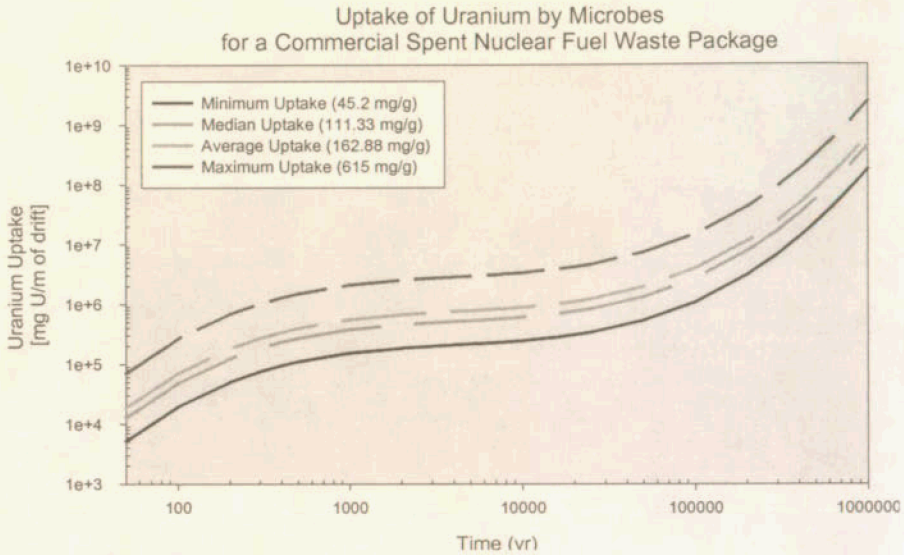

Figure 8

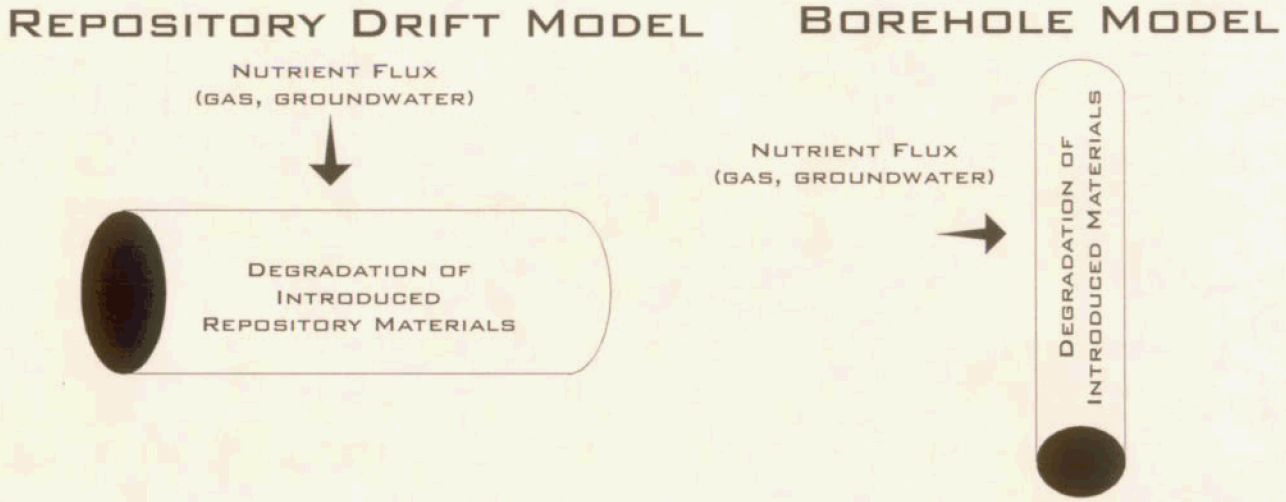

Figure 9